A Previously Unrecognized Monocytic Component of Pheochromocytoma and Paraganglioma

Nada A. Farhat[1] · James F. Powers[2] · Annette Shepard-Barry[2] · Patricia Dahia[3] · Karel Pacak[4] · Arthur S. Tischler[2]

Abstract

We describe a consistently present, previously unrecognized, population of monocytes in pheochromocytomas and paragangliomas. Although sustentacular cells are generally recognized as a common component of these tumors, differential immunohistochemical staining for CD163 and S100 shows that monocytes can in fact be more numerous. These cells frequently resemble sustentacular cells topographically and cytologically, possibly explaining why they have not been previously noticed. They contribute to the tumor proteome and may have implications for tumor biology. No correlations were identifiable between the presence of these cells and any clinical characteristics of the tumors in the present study. A possible association with genotype is suggested by immunoblot showing high expression of CD163 protein in tumors with succinate dehydrogenase mutations.

Keywords Pheochromocytoma · Paraganglioma · Monocyte · Macrophage · Sustentacular cell · Immunohistochemistry

Introduction

Pheochromocytomas (PCC) and paragangliomas (PGL) are closely related tumors of neural crest–derived neuroendocrine cells that arise principally along the paraxial distribution of sympathetic ganglia and nerve fibers and in association with branches of the vagus and glossopharyngeal nerves in the head and neck. According to the current WHO terminology, the term pheochromocytoma is reserved for PGL in the adrenal gland and PCC are considered as intra-adrenal PGL [1]. PCC/PGL have a strong hereditary predisposition. At least 30% of these tumors are now known to be hereditary, and at least 19 hereditary susceptibility genes are implicated in their development [2–4].

The neoplastic endocrine cells in PCC/PGL are known as chromaffin cells or chief cells. A second distinctive cell population, recognized by immunohistochemical staining for S100 protein, consists of sustentacular cells. Although their numbers vary, sustentacular cells are almost always found in PCC/PGL and their presence can be a useful, though not entirely reliable, aid in diagnosis. The origin and functions of sustentacular cells are unclear. Some studies suggest that they are non-neoplastic cells attracted to the tumors by chief cell-derived signals [5], while others suggest that they arise through divergent differentiation or may be neural crest stem cells [6].

In a recent tissue culture study, we serendipitously observed that numerous small cells accumulated in microwells containing explants of a PGL. Investigation, by immunohistochemical stains, revealed that these cells did not stain for S100 and were therefore not sustentacular cells. They were also negative for CD117 and were therefore not mast cells, which have been observed in small numbers in normal paraganglia [7]. In order to further pursue their identity, we stained sections of the PGL for other immunohistochemical markers and identified a dense population of cells positive for both CD163 and CD68, consistent with monocyte-macrophage lineage. Because monocytes have not previously been reported as a major component of PCC/PGL, we sought to determine their prevalence and distribution in a series of these tumors.

✉ James F. Powers
jpowers1@tuftsmedicalcenter.org

1   New York Eye and Ear Infirmary of Mount Sinai Icahn School of Medicine, New York, NY, USA

2   Department of Pathology and Laboratory Medicine, Tufts Medical Center, 800 Washington Street, Box 802, Boston, MA 02111, USA

3   Department of Medicine and Cellular and Structural Biology, University of Texas Health Science Center, San Antonio, TX, USA

4   Section on Medical Neuroendocrinology Eunice Kennedy Shriver National Institute of Child Health and Human Development (NICHD), National Institutes of Health, Bethesda, MD, USA

Materials and Methods

Tumor Sampling

Studies were initially performed on a tissue microarray (TMA) that consisted of 1 mm cores representing 52 sympathoadrenal PCC/PGL (48 adrenal PCC, 4 extra-adrenal abdominal PGL, 1 site unspecified). Patient ages ranged from 11 to 81 years and tumor sizes ranged from $2.0 \times 2.0 \times 2.0$ cm to $17.0 \times 14.0 \times 11.0$ cm. Ten tumors arose in patients with known germline mutations of PCC/PGL susceptibility genes (3 RET, 2 VHL, 2 SDHB, 1 SDHD, 1 NF1, and 1 MEN1). Forty-two tumors were apparently sporadic or not genetically tested. The array contained three tissue cores from each tumor as a means of assessing intratumoral heterogeneity. Lymph node and spleen tissue samples were included on the array as controls.

After analyzing the TMA, we additionally examined conventional histological sections representing five PCC and five PGL from different anatomic locations. This series was studied both for validation to confirm that TMA cores faithfully reflected findings in larger samples, and to determine whether sympathoadrenal PGL differed from PGL in other anatomic locations. In addition to staining for CD163 and S100, the ten representative tumors in this set were stained for CD117 to assess the number and distribution of mast cells.

Immunohistochemistry

Immunohistochemical staining for CD163, S100, and CD117 was performed using mouse monoclonal antibodies (Ventana, Tucson, AZ) after microwave antigen retrieval in citrate buffer, pH6. Antibodies were diluted in phosphate-buffered saline pH 7.4 containing a Ventana blocking solution. Dilutions were optimized for use on a Ventana automated slide stainer in combination with Ventana detection kits. Positive CD163 staining of tissue macrophages and S100 staining of sustentacular cells or nerve fibers provided positive internal controls in all sections that were considered interpretable. Negative controls substituting irrelevant mouse IgG for the primary antibodies were completely negative.

Analysis of Immunostaining

For quantitative analysis, all monocytes and sustentacular cells were counted in each tissue core on adjacent 5 μm microarray sections stained for CD163 and S100, respectively. Positivity for CD163 was defined as granular cytoplasmic or cytoplasmic and membrane staining. Positivity for S100 was defined by the presence of nuclear or nuclear plus cytoplasmic staining. Positive cells were counted via digital scan images using Aperio digital microscope (Spectrum Version 11.1.1.765) at × 20 magnification.

Because both monocytes and sustentacular cells extended short processes, only cells containing a nucleus within the plane of section were scored in order to avoid counting a cell more than once. Counts for each core were normalized per square millimeter, calculated from the 1 mm core diameter, to obtain numerical densities. Ratios of monocytes to sustentacular cells were also calculated.

For the ten whole slide surgical specimens of PCC/PGL, three fields with the highest density of staining for CD163 and S100 were selected from a slide representing each specimen. The ratios of CD163 and S100 positive cells were compared between the sets of PCC and PGL specimens.

In addition, the distribution of monocytes for each tumor was classified into one of three patterns: predominantly (> 70%) intra and/or perivascular, predominantly (> 70%) interstitial between tumor cells, or mixture of both intra or perivascular and interstitial.

Statistical Analysis

Numerical densities of monocytes and sustentacular cells and ratios of monocytes to sustentacular cells were calculated in each core of all tumors represented in the microarray. The data were analyzed for possible associations with tumor size, location and genotype, and with patient age and sex. In addition, patterns of monocyte distribution between cores of individual tumors were compared as a measure of intratumoral heterogeneity. To evaluate counts in relation to age, patients were divided into three intervals: < 30 years ($n = 10$), 31–60 years ($n = 21$), and > 61 years ($n = 14$). Statistical significance was assessed using an unpaired t test.

Immunoblots for CD163

An immunoblot of protein from nine representative tumors was probed for CD163 to test whether monocytes contribute substantially to the tumor proteome. This also served as a preliminary test for association with genotype, by including two tumors with SDHB mutations and one each with mutations of SDHC, SDHD, RET (MEN2A) VHL, and NF1. Two tumors were apparently sporadic. Methods for protein extraction, electrophoresis, and immunoblotting were as previously described by Powers et al. [8].

Results

Adjacent sections of a TMA with PCC/PGL samples from 52 patients were stained for S100 and CD163, with each tumor represented by three cores. Thirty-two randomly distributed cores were excluded for technical reasons affecting one or both stains, so that some tumors were represented by only one or two cores. This did not affect the overall study conclusions.

Prominent monocytes and sustentacular cells were observed in all tumors. However, marked intratumoral heterogeneity was evident, to the extent that exclusively CD163 or exclusively S100-stained cells were present in some of the cores. The patterns of distribution of the two cell types were often very similar or indistinguishable in that both could be found adjacent to capillaries at the periphery of tumor cell nests (zellballen) or interstitially. An exception was that monocytes could also be found adjacent to larger blood vessels (Fig. 1).

Pooled counts of all cores for each individual tumor were used to generate the average counts/mm^2 per tumor. Based on pooled counts of all cores for each individual tumor, including both PCC and PGL, monocyte counts based on CD163 stains revealed an average of 54.07 ± 4.8 cells/mm^2 per tumor ($n = 48$). Counts of sustentacular cells based on S100 stains revealed an average of only 13.01 ± 3.1 cells/mm^2 ($n = 52$), ($P < 0.0001$, unpaired t test). The ratio of monocytes to sustentacular cells among all tumors was 3.1:1. When PCC and PGL represented in the TMA were considered separately, the PCC averaged 54.76 ± 5.03 monocytes/mm^2 per tumor ($n = 34$), versus 11.79 ± 3.14 sustentacular cells/mm^2 per tumor ($n = 47$) for a ratio of 4.4:1 ($P < 0.0001$). In contrast, for PGL represented in the TMA ($n = 4$), the average numbers were 39.08 ± 19.13 monocytes and 29.4 ± 15.21 sustentacular cells cells/mm^2 per tumor ($P > 0.05$), for a ratio of 1.34:1.

There were no statistically significant differences detectable in relation to patients' gender, age, or mutation status. Although the monocyte to sustentacular cell ratio in patients < 30 years old was 2.9:1, versus 6.7:1 in patients between the ages of 31 and 60 years, the data were not statistically significant. Among the nine tumors in the TMA with known germline mutations, the average of CD163 to S100 positive cells ranged from 1:1 in the single tumor with germline *NF1* mutation to 11:1 and 22:1 in the two tumors with *VHL* and *RET* mutations, respectively.

In contrast to the TMA specimens, whole slide analysis of the 10 surgical specimens included in the study showed ratios of monocytes to sustentacular cells that were 1.6:1 in PCC and 0.7:1 in PGL ($P > 0.05$). The apparent discrepancy from the TMA results reflected the different sampling between the TMA, in which random areas determined by pre-existing cores were counted, compared to counting areas with densest labeling on the whole slides. Marked intratumoral heterogeneity, which was most obvious as areas of dense and sparse sustentacular cells, accounted for the lower proportion of monocytes.

Immunohistochemical examination of whole slide surgical specimens also revealed a range of relevant features not seen in the TMA, including one case with a very dramatic encirclement of zellballen by monocytes (Fig. 2) and one with an extremely dense accumulation of monocytes in normal adrenal cortex and medulla adjacent to a monocyte-sparse PCC (Fig. 3). These findings suggest the existence of possibly competing mechanisms for attracting monocytes to tumor cells—and denying them access. The variable presence of mast cells (Fig. 2) and macrophages (Figs. 2 and 4) was also confirmed.
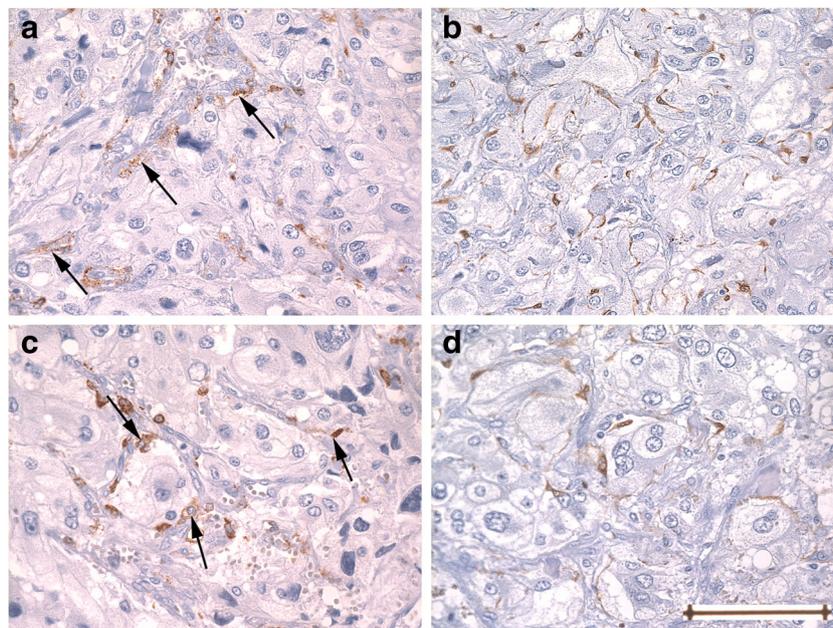

Fig. 1 Adjacent sections of tissue microarray showing representative patterns of staining for CD163 (**a**, **c**) and S-100 (**b**, **d**) as seen in two cores from a single tumor. Panels **a** and **b** are from one core, **c** and **d** from another. Cells immunoreactive for CD 163 (arrows) are predominantly perivascular in **a**, while in **c**, they are predominantly at the periphery of zellballen or, less often, interstitial (right arrow). The latter pattern resembles the distribution of sustentacular cells stained for S-100 seen in both cores. In contrast to cells staining for CD163, cells that stain for S-100 are found only in an interstitial/peripheral distribution and are not perivascular. Original magnification × 400, Bar = 100 μm

Fig. 2 Sections of a carotid PGL showing distributions of monocytes (**b**, CD163), sustentacular cells (**c**, S100) and mast cells (**d**, CD117). Note the pronounced partial encirclement of Zellballen by monocytes and the sparse, uneven distribution of mast cells
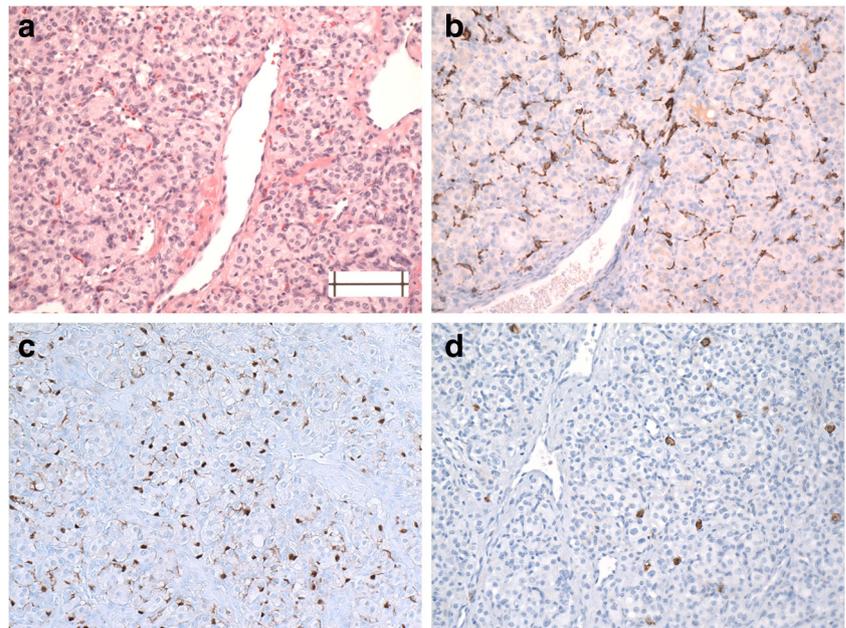
Immunoblotting for CD163 confirmed the consistent presence of CD163 protein and showed bands varying in intensity in all nine PCC and PGL studied. There was no detectable correlation with anatomic tumor location. However, the band intensity was least in tumors associated with germline *NF1* and *MEN2A* mutations and tended to be highest in those with *SDH* mutations (Fig. 5).

Discussion

To our knowledge, this brief report is the first to demonstrate that a substantial population of cells of monocyte/macrophage lineage is consistently present in pheochromocytomas and paragangliomas. This observation is potentially important for several reasons. First, in the era of sensitive multi-omic tumor profiling [9], the contributions of different populations of normal and neoplastic cells within a given tumor must be resolved. Second, because monocytes in PCC/PGL may

Fig. 3 Adjacent sections of normal adrenal adjacent to a pheochromocytoma (**a** H&E; **b** CD163). From left to right, both panels show zona fasciculata, zona reticularis, a small amount of normal adrenal medulla, and pheochromocytoma. Only occasional scattered monocytes similar to those in Fig. 1 are present in the tumor, while numerous monocytes and macrophages have accumulated in the normal tissue
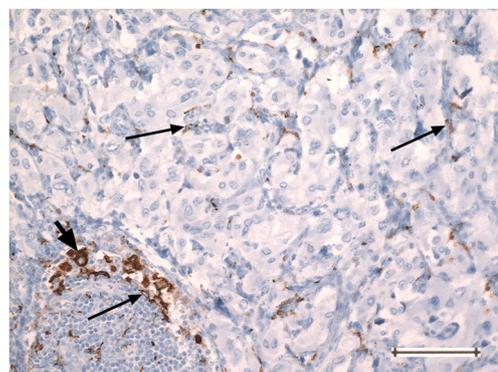

Fig. 4 PGL showing a CD163-positive macrophage (thick arrow, at left) in an uncommon area of lymphocytic inflammation. The cell size and nuclear size of the macrophage are greater than those of the small CD163-positive monocytes with slender processes (thin arrows) present throughout the tumor. Original magnification × 200. Bar = 100 μm
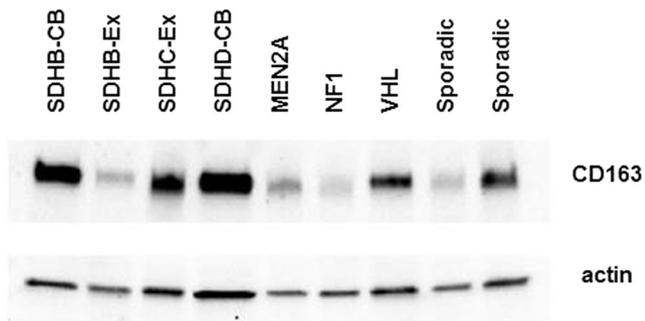
Fig. 5 Immunoblot confirming the presence of CD163 in five representative PCC and four extra-adrenal PGL (CB, carotid body; Ex, extra-adrenal abdominal). CD163 is readily detectable in all of the tumors, regardless of genotype, but there is marked intertumoral variation. Lane 1 represents the tumor stained immunohistochemically in Fig. 2

resemble sustentacular cells in shape and topographical distribution, possibly explaining why they have not been previously noticed, care must be taken to not mistake the two cell types in immunohistochemical stains, e.g., for SDHB or SDHA [10]. Finally, and perhaps most importantly, intratumoral monocytes represent a reserve of potential antigen-presenting cells [11] that might suggest new approaches to immunotherapy. Although PCC/PGL have an extremely low mutational burden [9], and therefore low immunogenicity, immunotherapy has been considered as a potential treatment for patients with metastases from these tumors, and a clinical trial (No. 2015-0948) of the PD-1 (programmed cell death protein 1) inhibitor pembrolizumab is currently open to patients.

Because of intratumoral heterogeneity and the small sample size in this study, we were not able to ascertain whether there are meaningful differences in monocyte content or ratio of monocytes to sustentacular cells between PCC/PGL from various anatomic locations using differential cell counts. Nor were we able to establish correlations with patients' age, sex, or genotype. These questions, especially the influence of genotype, require further investigation. The number of hereditary cases in this study was smaller than expected, probably because of incomplete testing of older cases represented in the microarray. However, an intriguing finding related to genotype was that three of the four tumors with mutations of genes encoding succinate dehydrogenase subunits showed the highest levels of CD163 on an immunoblot. While this finding is of unclear significance because of small sample size and requires extensive confirmatory study, it is highly consistent with the recent discovery that inhibition of succinate dehydrogenase, which constitutes mitochondrial complex II, facilitates hypoxic gene expression in monocytes [12]. Further, "metabolic rewiring" of monocytes, with increased synthesis of succinate, takes place during the deactivation of monocytes recovering from a response to sepsis [13]. These metabolic processes may hold clues to the utilization of resident monocytes in treatment strategies.

References

1. Lloyd R, Osamura R, Klöppel G, Rosai J (eds) (2017) WHO Classification of Tumours of Endocrine Organs, Fourth Edition, vol 10. IARC
2. Gimenez-Roqueplo AP, Dahia PL, Robledo M (2012) An update on the genetics of paraganglioma, pheochromocytoma, and associated hereditary syndromes. Horm Metab Res 44 (5):328–333. doi: https://doi.org/10.1055/s-0031-1301302
3. Dahia PL (2014) Pheochromocytoma and paraganglioma pathogenesis: learning from genetic heterogeneity. Nature reviews Cancer 14 (2):108–119. doi:https://doi.org/10.1038/nrc3648
4. Papathomas TG, Giordano TJ, Maher ER, Tischler AS (2019) Adrenal Glands Tumors: Pathology and Genetics. In: Boffetta P, Hainaut P (eds) Encyclopedia of Cancer, vol 1. 3rd edn. Elsevier, Academic Press, pp 18–29. doi:https://doi.org/10.1016/B978-0-12-801238-3.65087-0
5. Douwes Dekker PB, Corver WE, Hogendoorn PC, van der Mey AG, Cornelisse CJ (2004) Multiparameter DNA flow-sorting demonstrates diploidy and SDHD wild-type gene retention in the sustentacular cell compartment of head and neck paragangliomas: chief cells are the only neoplastic component. J Pathol 202 (4):456–462
6. Lopez-Barneo J (2018) Oxygen sensing and stem cell activation in the hypoxic carotid body. Cell Tissue Res. doi:https://doi.org/10.1007/s00441-017-2783-9, 372, 417, 425
7. Kraus R, Bezdicek P (1988) The incidence of mastocytes in paraganglia. Folia morphologica 36 (2):211–213
8. Powers JF, Brachold JM, Tischler AS (2003) Ret protein expression in adrenal medullary hyperplasia and pheochromocytoma. Endocr Pathol 14 (4):351–361
9. Fishbein L, Leshchiner I, Walter V, Danilova L, Robertson AG, Johnson AR, Lichtenberg TM, Murray BA, Ghayee HK, Else T, Ling S, Jefferys SR, de Cubas AA, Wenz B, Korpershoek E, Amelio AL, Makowski L, Rathmell WK, Gimenez-Roqueplo AP, Giordano TJ, Asa SL, Tischler AS, Cancer Genome Atlas Research N, Pacak K, Nathanson KL, Wilkerson MD (2017) Comprehensive Molecular Characterization of Pheochromocytoma and Paraganglioma. Cancer Cell 31 (2):181–193. doi:https://doi.org/10.1016/j.ccell.2017.01.001
10. Papathomas TG, Oudijk L, Persu A, Gill AJ, van Nederveen F, Tischler AS, Tissier F, Volante M, Matias-Guiu X, Smid M,

Favier J, Rapizzi E, Libe R, Curras-Freixes M, Aydin S, Huynh T, Lichtenauer U, van Berkel A, Canu L, Domingues R, Clifton-Bligh RJ, Bialas M, Vikkula M, Baretton G, Papotti M, Nesi G, Badoual C, Pacak K, Eisenhofer G, Timmers HJ, Beuschlein F, Bertherat J, Mannelli M, Robledo M, Gimenez-Roqueplo AP, Dinjens WN, Korpershoek E, de Krijger RR (2015) SDHB/SDHA immunohistochemistry in pheochromocytomas and paragangliomas: a multicenter interobserver variation analysis using virtual microscopy: a Multinational Study of the European Network for the Study of Adrenal Tumors (ENS@T). Modern pathology : an official journal of the United States and Canadian Academy of Pathology, Inc 28 (6):807–821. doi:https://doi.org/10.1038/modpathol.2015.41

11. Jakubzick CV, Randolph GJ, Henson PM (2017) Monocyte differentiation and antigen-presenting functions. Nat Rev Immunol 17 (6):349–362. doi:https://doi.org/10.1038/nri.2017.28

12. Sharma S, Wang J, Cortes Gomez E, Taggart RT, Baysal BE (2017) Mitochondrial complex II regulates a distinct oxygen sensing mechanism in monocytes. Hum Mol Genet 26 (7):1328–1339. doi: https://doi.org/10.1093/hmg/ddx041

13. Zhu X, Meyers A, Long D, Ingram B, Liu T, Yoza BK, Vachharajani V, McCall CE (2019) Frontline Science: Monocytes sequentially rewire metabolism and bioenergetics during an acute inflammatory response. J Leukoc Biol 105 (2):215–228. doi: https://doi.org/10.1002/JLB.3HI0918-373R